MOTION IDENTIFICATION OF PLANAR FREE-FORM OBJECTS

Mustafa Unel
Faculty of Engineering and Natural Sciences
Sabanci University
Orhanli-Tuzla 34956, Istanbul, Turkey
email: munel@sabanciuniv.edu

B. K. Ghosh
Department of Electrical and Systems Engineering
Washington University
St. Louis, MO 63130, USA
email: ghosh@netra.wustl.edu

ABSTRACT
It has been shown recently that rigid or affine dynamics of curves defined by algebraic equations can be represented in terms of Riccati dynamics of possibly complex lines. In this work, we develop new Riccati equations in real variables for closed-bounded curves and new recursions on multiplicative scalars in the decomposition of the curve. A parameter identification scheme has also been proposed, and the results are verified by simulations.

KEY WORDS
Algebraic Curves, Rigid and Affine Dynamics, Riccati Equations, Parameter Identification.

1 Introduction

Algebraic curves and surfaces have been used in various branches of engineering for a long time, but in the past two decades they have proven very useful in many model-based applications. Various algebraic and geometric invariants obtained from implicit models of curves and surfaces have been studied rather extensively in Computer Vision, especially for single computation pose estimation, shape tracking, 3D surface estimation from multiple images and efficient geometric indexing of large pictorial databases [1]-[11].

In an earlier paper [6], we have shown that rigid or affine dynamics of curves defined by implicit polynomial equations can be represented in terms of Riccati dynamics of possibly complex lines. The application of this result was illustrated for planar curves moving in $\mathbb{R}^3$ and for the perspective projections of these curves on the image plane of a CCD camera. In this paper, we develop new Riccati equations in real variables for closed-bounded curves and obtain some new recursions on parameters. We also propose a parameter identification scheme for estimating the rigid motion parameters of a free-form curve. We illustrate the validity of our proposed approach by simulations. There has been a steadily growing literature in robotics on the problem of line correspondence for line features moving in $\mathbb{R}^3$, (see [12]- [16]). For some other older references in the literature on the dynamics of curves, see [17]- [19].

2 Algebraic Curves

Algebraic curves are defined by implicit equations of the form $f_n(x,y) = 0$, where $f_n(x,y)$ is a polynomial in the variables x, y, i.e. $f_n(x,y) = \sum_{ij} a_{ij} x^i y^j$ where $0 \leq i+j \leq n$ (n is finite) and the coefficients a_{ij} are real numbers [1]. A monic polynomial $f_n(x,y) = 0$ will be defined by the condition that $a_{n0} = 1$. Algebraic curves of degree $1, 2, 3, 4, \ldots$ are called *lines, conics, cubics, quartics, ...*etc. Fig. 1 depicts the boundaries of several two-dimensional *free-form* objects with superimposed quartic algebraic curves.

In the sequel, we will restrict our attention to quartic curves and note that the results can easily be generalized to higher degree curves.

3 Decomposed Quartics and Riccati Equations

As detailed in [4], algebraic curves can be decomposed as a *unique* sum of *line products*. Example of a quartic decomposition in terms of 6 complex lines is geometrically shown in Fig. 2.

In [6], we considered a line decomposed planar quartic curve

$$f_4(x,y) = \prod_{i=1}^{4} \begin{pmatrix} 1 & l_{4i} & k_{4i} \end{pmatrix} \begin{pmatrix} x \\ y \\ 1 \end{pmatrix} + \alpha \prod_{i=1}^{2} \begin{pmatrix} 1 & l_{2i} & k_{2i} \end{pmatrix} \begin{pmatrix} x \\ y \\ 1 \end{pmatrix} + \beta = 0 \qquad (1)$$

and its homogenized version, namely

$$f_4(\bar{x},\bar{y},\bar{w}) = \prod_{i=1}^{4} \begin{pmatrix} \bar{p}_i & \bar{l}_{4i} & \bar{k}_{4i} \end{pmatrix} \begin{pmatrix} \bar{x} \\ \bar{y} \\ \bar{w} \end{pmatrix} + \alpha \bar{w}^2 \frac{\prod_{i=1}^{4} \bar{p}_i}{\prod_{i=1}^{2} \bar{q}_i} \prod_{i=1}^{2} \begin{pmatrix} \bar{q}_i & \bar{l}_{2i} & \bar{k}_{2i} \end{pmatrix} \begin{pmatrix} \bar{x} \\ \bar{y} \\ \bar{w} \end{pmatrix} + \beta \bar{w}^4 \prod_{i=1}^{4} \bar{p}_i = 0 \qquad (2)$$

obtained from (1) by using the following substitutions:

$$x = \frac{\bar{x}}{\bar{w}}, \;\; y = \frac{\bar{y}}{\bar{w}}, \;\; l_{4i} = \frac{\bar{l}_{4i}}{\bar{p}_i}, \;\; k_{4i} = \frac{\bar{k}_{4i}}{\bar{p}_i},$$

$$l_{2i} = \frac{\bar{l}_{2i}}{\bar{q}_i}, \;\; k_{2i} = \frac{\bar{k}_{2i}}{\bar{q}_i} \qquad (3)$$

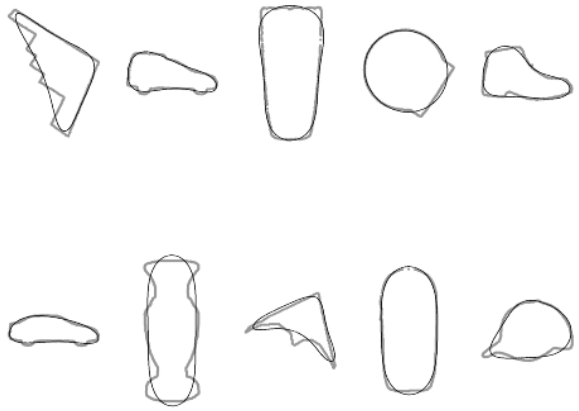

Figure 1. A group of Free-Form Quartic Curves as Outlines of 2D Objects: examples include a plane, a van, a glass vaze, a CD box, a shoe, a car, another vaze, a glider, a cellular phone, and a hat in above order

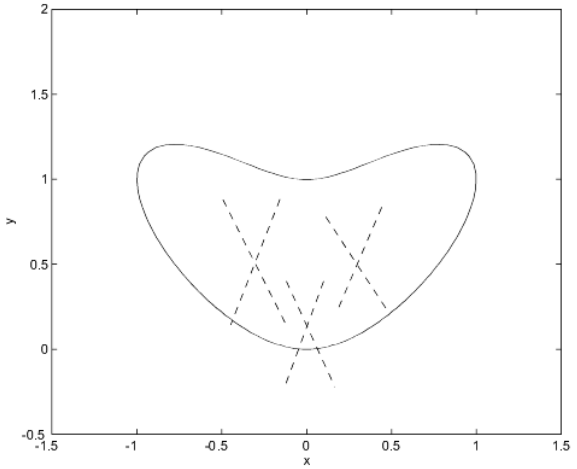

Figure 2. A Boomerang Shaped Curve (Solid) and its Complex Line Factors (Dashed)

Let us now consider an affine motion in the cartesian and in the homogeneous coordinates as follows:

$$\frac{d}{dt}\begin{pmatrix} x \\ y \\ 1 \end{pmatrix} = \underbrace{\begin{pmatrix} a_1 & a_2 & b_1 \\ a_3 & a_4 & b_2 \\ 0 & 0 & 0 \end{pmatrix}}_{A}\begin{pmatrix} x \\ y \\ 1 \end{pmatrix} \Rightarrow$$

$$\frac{d}{dt}\begin{pmatrix} \bar{x} \\ \bar{y} \\ \bar{w} \end{pmatrix} = \underbrace{\begin{pmatrix} a_1 & a_2 & b_1 \\ a_3 & a_4 & b_2 \\ 0 & 0 & 0 \end{pmatrix}}_{A}\begin{pmatrix} \bar{x} \\ \bar{y} \\ \bar{w} \end{pmatrix} \qquad (4)$$

We obtain the following dynamics on the line parameters and on the coefficients $\alpha(t)$ and $\beta(t)$:

$$\frac{d}{dt}\begin{pmatrix} \bar{p}_i(t) \\ \bar{l}_{4i}(t) \\ \bar{k}_{4i}(t) \end{pmatrix} = -A^T\begin{pmatrix} \bar{p}_i(t) \\ \bar{l}_{4i}(t) \\ \bar{k}_{4i}(t) \end{pmatrix} =$$

$$\begin{pmatrix} -a_1 & -a_3 & 0 \\ -a_2 & -a_4 & 0 \\ -b_1 & -b_2 & 0 \end{pmatrix}\begin{pmatrix} \bar{p}_i(t) \\ \bar{l}_{4i}(t) \\ \bar{k}_{4i}(t) \end{pmatrix} \;\; i = 1,2,3,4 \qquad (5)$$

$$\frac{d}{dt}\begin{pmatrix} \bar{q}_i(t) \\ \bar{l}_{2i}(t) \\ \bar{k}_{2i}(t) \end{pmatrix} = -A^T\begin{pmatrix} \bar{q}_i(t) \\ \bar{l}_{2i}(t) \\ \bar{k}_{2i}(t) \end{pmatrix} =$$

$$\begin{pmatrix} -a_1 & -a_3 & 0 \\ -a_2 & -a_4 & 0 \\ -b_1 & -b_2 & 0 \end{pmatrix}\begin{pmatrix} \bar{q}_i(t) \\ \bar{l}_{2i}(t) \\ \bar{k}_{2i}(t) \end{pmatrix} \;\; i = 1,2. \qquad (6)$$

$$\alpha(t) = (\prod_{i=1}^{4}\frac{\bar{p}_i(0)}{\bar{p}_i(t)})(\prod_{i=1}^{2}\frac{\bar{q}_i(t)}{\bar{q}_i(0)})\alpha(0); \qquad (7)$$

$$\beta(t) = (\prod_{i=1}^{4}\frac{\bar{p}_i(0)}{\bar{p}_i(t)})\beta(0). \qquad (8)$$

3.1 Riccati Equations

By differentiating (3) with respect to time and using (5) and (6), it has also been shown in [6] that line parameters $l_{4i}, k_{4i}, l_{2i}, k_{2i}$ in the decomposition of the original curve satisfy coupled Riccati equations, namely

$$\dot{l}_{4i} = -a_2 + (a_1 - a_4)l_{4i} + a_3 l_{4i}^2, \;\; i = 1,2,3,4 \qquad (9)$$

$$\dot{k}_{4i} = -b_1 - b_2 l_{4i} + a_1 k_{4i} + a_3 l_{4i} k_{4i}, \;\; i = 1,2,3,4 \qquad (10)$$

$$\dot{l}_{2i} = -a_2 + (a_1 - a_4)l_{2i} + a_3 l_{2i}^2, \;\; i = 1,2 \qquad (11)$$

$$\dot{k}_{2i} = -b_1 - b_2 l_{2i} + a_1 k_{2i} + a_3 l_{2i} k_{2i}, \;\; i = 1,2 \qquad (12)$$

Note that the line parameters, i.e. slope and intercept, satisfy coupled Riccati equations with parameters that depend on the motion of the curve. Note also that each of the lines satisfies the same Riccati Equation initialized at different points on the state space.

3.2 Riccati Equations in Real Variables for Closed-Bounded Quartics

For a closed-bounded quartic curve, l_{4i} and k_{4i} have to be complex. Focusing on these:

$$l_{4i} = \eta_{1i} + j\eta_{2i}, \;\; k_{4i} = \eta_{3i} + j\eta_{4i} \qquad (13)$$

where $\eta_{1i} = Re(l_{4i})$, $\eta_{2i} = Im(l_{4i})$, $\eta_{3i} = Re(k_{4i})$, $\eta_{4i} = Im(k_{4i})$. Substituting these into (9) and (10),

$$\dot{l}_{4i} = \dot{\eta}_{1i} + j\dot{\eta}_{2i} = -a_2 + (a_1 - a_4)(\eta_{1i} + j\eta_{2i}) + a_3(\eta_{1i} + j\eta_{2i})^2$$

$$\Rightarrow \dot{\eta}_{1i} + j\dot{\eta}_{2i} = -a_2 + (a_1 - a_4)\eta_{1i} + a_3({\eta_{1i}}^2 - {\eta_{2i}}^2) + j[(a_1 - a_4)\eta_{2i} + 2a_3\eta_{1i}\eta_{2i}]$$

Equating the real and the imaginary parts we obtain the following:

$$\dot{\eta}_{1i} = -a_2 + (a_1 - a_4)\eta_{1i} + a_3({\eta_{1i}}^2 - {\eta_{2i}}^2) \quad (14)$$

$$\dot{\eta}_{2i} = (a_1 - a_4)\eta_{2i} + 2a_3\eta_{1i}\eta_{2i} \quad (15)$$

Similarly, we also have the following

$$\dot{k}_{4i} = \dot{\eta}_{3i} + j\dot{\eta}_{4i} = -b_1 - b_2(\eta_{1i} + j\eta_{2i}) + a_1(\eta_{3i} + j\eta_{4i}) + a_3(\eta_{1i} + j\eta_{2i})(\eta_{3i} + j\eta_{2i})$$

$$\dot{\eta}_{3i} + j\dot{\eta}_{4i} = -b_1 - b_2\eta_{1i} + a_1\eta_{3i} + a_3(\eta_{1i}\eta_{3i} - \eta_{2i}\eta_{4i}) + j[-b_2\eta_{2i} + a_1\eta_{4i} + a_3(\eta_{1i}\eta_{4i} + \eta_{2i}\eta_{3i})]$$

As before, equating the real and the imaginary parts we have

$$\dot{\eta}_{3i} = -b_1 - b_2\eta_{1i} + a_1\eta_{3i} + a_3(\eta_{1i}\eta_{3i} - \eta_{2i}\eta_{4i}) \quad (16)$$

$$\dot{\eta}_{4i} = -b_2\eta_{2i} + a_1\eta_{4i} + a_3(\eta_{1i}\eta_{4i} + \eta_{2i}\eta_{3i}) \quad (17)$$

3.3 Recursion on Parameters

In light of (5) and (6),

$$\dot{\bar{p}}_i(t) = -a_1\bar{p}_i(t) - a_3\bar{l}_{4i}(t) \Rightarrow$$

$$\frac{\dot{\bar{p}}_i(t)}{\bar{p}_i(t)} = -a_1 - a_3\underbrace{\frac{\bar{l}_{4i}(t)}{\bar{p}_i(t)}}_{l_{4i}(t)} = -a_1 - a_3 l_{4i}(t)$$

Integrating both sides we have

$$\ln(\bar{p}_i(\mu))]_0^t = -\int_0^t (a_1 + a_3 l_{4i}(\mu))d\mu \Rightarrow$$

$$\frac{\bar{p}_i(t)}{\bar{p}_i(0)} = e^{-\int_0^t (a_1 + a_3 l_{4i}(\mu))d\mu}$$

Similarly, from (6) we get

$$\frac{\bar{q}_i(t)}{\bar{q}_i(0)} = e^{-\int_0^t (a_1 + a_3 l_{2i}(\mu))d\mu}$$

Finally from (7), (8) we conclude that

$$\alpha(t) = \left(\frac{\prod_{i=1}^4 e^{\int_0^t (a_1 + a_3 l_{4i}(\mu))d\mu}}{\prod_{i=1}^2 e^{\int_0^t (a_1 + a_3 l_{4i}(\mu))d\mu}}\right)\alpha(0) =$$

$$e^{2a_1 t} e^{a_3 \int_0^t [\sum_{i=1}^4 l_{4i}(\mu) - \sum_{i=1}^2 l_{2i}(\mu)]d\mu}\alpha(0)$$

and

$$\beta(t) = \left(\prod_{i=1}^4 e^{\int_0^t (a_1 + a_3 l_{4i}(\mu))d\mu}\right)\beta(0)$$

$$= e^{4a_1 t} e^{a_3 \int_0^t [\sum_{i=1}^4 l_{4i}(\mu)]d\mu}\beta(0) \quad (18)$$

Equation (18) can be written in the form of an ordinary differential equation as follows:

$$\dot{\alpha} = [2a_1 + a_3(\sum_{i=1}^4 l_{4i}(t) - \sum_{i=1}^2 l_{2i}(t))]\,\alpha$$

$$\dot{\beta} = [4a_1 + a_3(\sum_{i=1}^4 l_{4i}(t))]\,\beta$$

4 Identification of Motion Parameters

Using vector-matrix notation and dropping the subscript i, equations (14) to (17) for a specific complex conjugate line pair can be recast as

$$\begin{pmatrix} \dot{\eta}_1 \\ \dot{\eta}_2 \\ \dot{\eta}_3 \\ \dot{\eta}_4 \end{pmatrix} = \begin{pmatrix} (a_1 - a_4) & 0 & 0 & 0 \\ 0 & (a_1 - a_4) & 0 & 0 \\ -b_2 & 0 & a_1 & 0 \\ 0 & -b_2 & 0 & a_1 \end{pmatrix} \begin{pmatrix} \eta_1 \\ \eta_2 \\ \eta_3 \\ \eta_4 \end{pmatrix} + a_3 \begin{pmatrix} {\eta_1}^2 - {\eta_2}^2 \\ 2\eta_1\eta_2 \\ \eta_1\eta_3 - \eta_2\eta_4 \\ \eta_1\eta_4 + \eta_2\eta_3 \end{pmatrix} + \begin{pmatrix} a_2 \\ 0 \\ b_1 \\ 0 \end{pmatrix}(-1) \quad (19)$$

which is a nonlinear plant of the form

$$\dot{X}_p = A_p X_p + C_p f(X_p) + B_p g(u) \quad (20)$$

where A_p, B_p and C_p are unknown constant matrices, $f(.)$ and $g(.)$ are known smooth functions of their arguments. Note in particular that $g(u) = -1$ is constant in our problem. To estimate the unknown parameters, we construct an estimator of the form [20]

$$\dot{\hat{X}}_p = A_m\hat{X}_p + (\hat{A}_p(t) - A_m)X_p + \hat{C}_p(t)f(X_p) + \hat{B}_p(t)g(u) \quad (21)$$

If the state error and parameter errors are defined as

$$e(t) \stackrel{def}{=} \hat{X}_p(t) - X_p(t), \;\; \Phi(t) \stackrel{def}{=} \hat{A}_p(t) - A_p,$$

$$\Psi(t) \stackrel{def}{=} \hat{C}_p(t) - C_p, \;\; \Gamma(t) \stackrel{def}{=} \hat{B}_p(t) - B_p,$$

then the error equations are given by

$$\dot{e}(t) = A_m e(t) + \Phi(t)X_p(t) + \Psi(t)f(X_p) + \Gamma(t)g(u), \quad (22)$$

where A_m is a stability matrix. The problem is to adjust the elements of the matrices $\hat{A}_p(t), \hat{C}_p(t)$ and $\hat{B}_p(t)$ or equivalently $\Phi(t), \Psi(t)$ and $\Gamma(t)$ so that the quantities $e(t), \Phi(t), \Psi(t), \Gamma(t)$ tend to zero as $t \to \infty$. We choose the adaptive laws to be

$$\dot{\hat{A}}_p(t) = \dot{\hat{\Phi}}(t) = -Pe(t)X_p^T(t)$$

$$\dot{\hat{C}}_p(t) = \dot{\hat{\Psi}}(t) = -Pe(t)f^T(X_p)$$

$$\dot{\hat{B}}_p(t) = \dot{\hat{\Gamma}}(t) = -Pe(t)g^T(u)$$

where P is a symmetric positive-definite matrix ($P > 0$), which satisfies the Lyapunov equation, namely

$$A_m^T P + PA_m = -Q$$

where Q is a positive-definite matrix ($Q > 0$). These laws can be used to ensure the global stability of the overall system with the output error tending to zero asymptotically. However, Lyapunov stability analysis only assures the asymptotic convergence of the state error to zero. The convergence of the parameters to their true values depends on the persistence excitation of the input u.

5 Simulation Results

In this section we show by simulations that starting from a sequence of curves, one can identify rigid motion parameters by decomposing the curves and using the Riccati Equations along with coefficient dynamics. Since the decomposition is essentially noisy with quantization and segmentation errors, it would be nice to see how good the motion parameters are estimated in presence of noise.

Free-form curves (objects) undergoing some 3D rigid motion in a fixed plane at a relatively large distance $Z = Z_0$ from a camera have been used to generate data on the image plane of the camera. This fixed plane is assumed to be perpendicular to the camera optical axis. So the camera effectively performs a scaled orthographic projection of object boundary data. That is the camera space variables can be expressed in terms of actual 3D position variables by:

$$x = \frac{f}{Z_0}X, \;\; y = \frac{f}{Z_0}Y \tag{23}$$

where f is the focal length of the camera, x, y are the image plane coordinate variables, and X, Y are the actual 3D space variables. Thus the related dynamics are $\dot{x} = \frac{f}{Z_0}\dot{X}$ and $\dot{y} = \frac{f}{Z_0}\dot{Y}$, which can be rearranged according to equation (4) by also using (23) as:

$$\begin{pmatrix} \dot{x} \\ \dot{y} \end{pmatrix} = \begin{pmatrix} 0 & \omega \\ -\omega & 0 \end{pmatrix} + \frac{f}{Z_0}\begin{pmatrix} b_1 \\ b_2 \end{pmatrix} \tag{24}$$

As a result the image data undergoes the same rotation as the actual data, but its translation parameters are scaled by $\frac{f}{Z_0}$ to reflect the effect of scaled orthographic projection. The resulting projected data are also corrupted by an additive noise of zero mean and $\sigma = 0.005$ standard deviation to model the effect of quantization errors. Image data so generated are then modelled by fitting closed-bounded quartic curves, at each sampling instant, using the fitting procedure detailed in [21]. Resulting quartic curves are then decomposed using the unique decomposition theorem of section 3 to obtain line parameters at each sampling instant. We picked one complex conjugate pair to construct

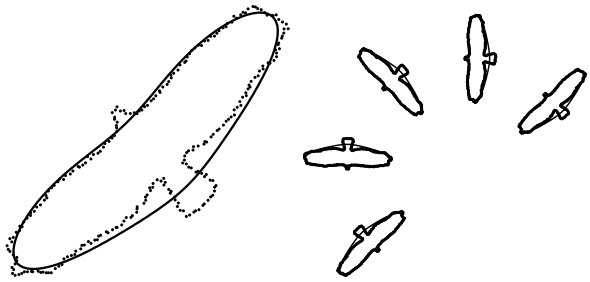

Figure 3. A Flight bird and its rigid motion

the dynamical system given by (19) and the estimator given by (21) in Matlab. Then the obtained dynamics are re-scaled in parallel with (24) for achieving the actual motion parameters in 3D. Accordingly, the rotational motion parameter in image plane is directly applied to get the actual rotation in 3D space, while the translation parameters are divided by $\frac{f}{Z_0}$.

To establish the correct correspondence between complex conjugate line pairs in consecutive curves, real intersection points (related-points) of these complex lines are determined and used in the evaluation of defining polynomials. It is known that the correct correspondence between two sets of related-points can be established by ordering the values of defining polynomials evaluated at these related-points [4].

The stability matrix, A_m and the positive-definite matrix Q are chosen to be:

$$A_m = \begin{pmatrix} -0.5 & 0 & 0 & 0 \\ 0 & -0.5 & 0 & 0 \\ 0 & 0 & -1.0 & 0 \\ 0 & 0 & 0 & -1.0 \end{pmatrix},$$

$$Q = \begin{pmatrix} 0.5 & 0 & 0 & 0 \\ 0 & 1.0 & 0 & 0 \\ 0 & 0 & 2.0 & 0 \\ 0 & 0 & 0 & 3.0 \end{pmatrix}$$

The Lyapunov equation is solved to determine the symmetric positive-definite matrix P, which is then used in parameter update rules given in section 4. Initial values of the motion parameters are chosen at random.

A flight bird employed in simulations and its rigid motion are depicted in Fig. 3 along with superimposed quartic curves. The actual 3D motion parameters of this object are $a_1 = a_4 = 0, \;\; a_2 = -a_3 = \omega = \pi/2, \;\; b_1 = -3, \;\; b_2 = 4$ for which the above estimation procedure is applied by shifting to camera plane, and then re-scaling for the actual motion parameters. Estimated parameters are plotted against time in Fig. 4. Note that estimated parameters converge to their true values with reasonably small estimation error.

A glider and its rigid motion are depicted in Fig. 5 along with superimposed quartic curves. The parameters of the actual rigid motion are $a_1 = a_4 = 0, \;\; a_2 = -a_3 =$

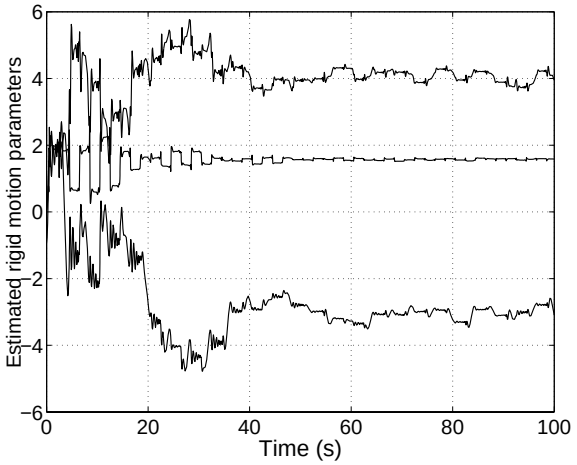

Figure 4. Estimated parameters versus Time. True parameters are $\omega = \pi/2$, $b_1 = -3$ and $b_2 = 4$

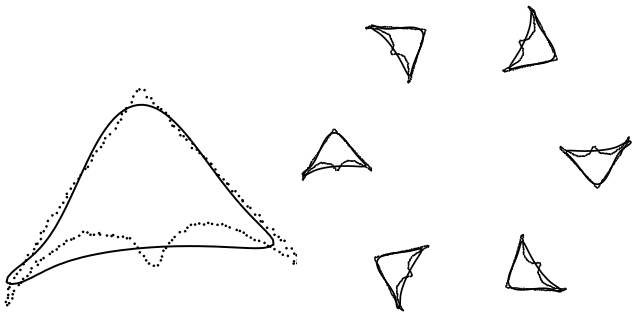

Figure 5. A Glider and its rigid motion

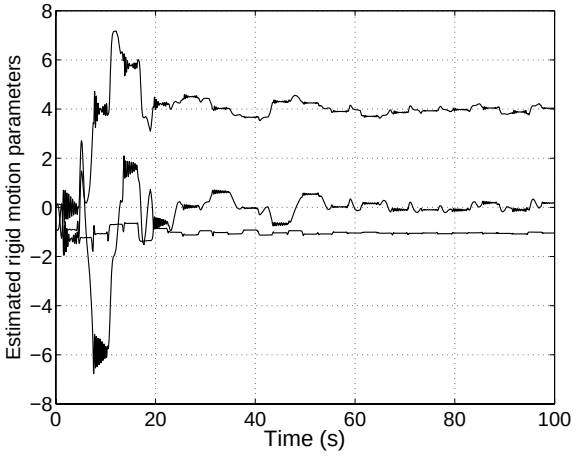

Figure 6. Estimated parameters versus Time. True parameters are $\omega = -\pi/3$, $b_1 = 4$ and $b_2 = 0$

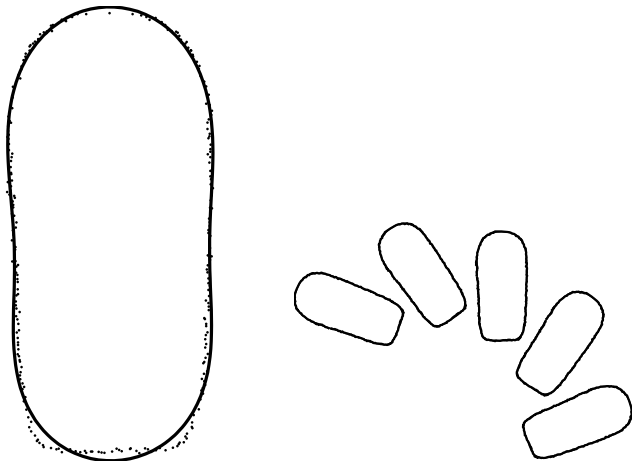

Figure 7. A Cellular Phone and its rigid motion

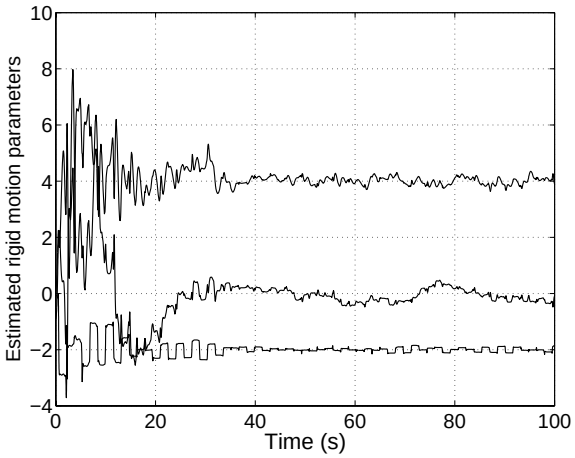

Figure 8. Estimated parameters versus Time. True parameters are $\omega = -2$, $b_1 = 4$ and $b_2 = 0$

$\omega = -\pi/3, \quad b_1 = 0, \quad b_2 = 4$. Estimated parameters are plotted against time in Fig. 6. Note again that estimates converge to their true values in a relatively short time interval with a relatively small estimation error.

Finally, a mobile cellular phone and its rigid motion are shown in Fig. 7. Motion parameters are $a_1 = a_4 = 0, \quad a_2 = -a_3 = \omega = -2, \quad b_1 = 4, \quad b_2 = 0$. Estimated parameters are plotted against time in Fig. 8. Notice the quick convergence and small estimation errors.

6 Conclusion

We have obtained new Riccati equations in real variables which can be used for estimating the motion parameters of a free-form closed-bounded curve undergoing rigid and affine motion. We have also proposed an identification/estimation scheme for estimating rigid motion parameters. Simulation results have shown that the rigid mo-

tion parameters of a free-form curve can accurately be estimated under noisy conditions. We are working on possible extensions of our estimation technique to affine and other motions as well.

7 Acknowledgements

The first author would like to thank Mr. Turker Sahin for performing the simulations of this work. The second author would like to acknowledge the support from NSF grants ECS-9976174, and ECS-0323693.

References

[1] C.G. Gibson, *Elementary geometry of algebraic curves*, (Cambridge University Press, Cambridge, UK, 1998).

[2] J. Bloomenthal, *Introduction to implicit surfaces*, (Kaufmann, Los Altos, CA, 1997).

[3] D. Keren et al., Fitting curves and surfaces to data using constrained implicit polynomials, *IEEE Transactions on Pattern Analysis and Machine Intelligence*, Vol. 23, No. 1, January 1999.

[4] M. Unel, W. A. Wolovich, On the construction of complete sets of geometric invariants for algebraic curves, *Advances in Applied Mathematics*, Vol. 24, No. 1, January 2000, 65-87.

[5] M. Unel, W. A. Wolovich, A new representation for quartic curves and complete sets of geometric invariants, *International Journal of Pattern Recognition and Artificial Intelligence*, December 1999.

[6] M. Unel, B. K. Ghosh, Dynamic Models of Planar Algebraic Curves, *Proceedings of IEEE CDC 2001*, December 2001.

[7] J. L. Mundy, Andrew Zisserman, *Geometric invariance in computer vision*, (The MIT Press, 1992).

[8] G. Taubin, D. B. Cooper, Symbolic and Numerical Computation for Artificial Intelligence, *2D and 3D object recognition and positioning with algebraic invariants and covariants*, (Academic Press, 1992).

[9] G. Taubin, F. Cukierman, S. Sullivan, J. Ponce and D.J. Kriegman, Parameterized families of polynomials for bounded algebraic curve and surface fitting, *IEEE Transactions on Pattern Analysis and Machine Intelligence*, March 1994.

[10] W. A. Wolovich, Mustafa Unel, The determination of implicit polynomial canonical curves, *IEEE Transactions on Pattern Analysis and Machine Intelligence*, Vol. 20, No. 10, October 1998, 1080-1089.

[11] W. A. Wolovich, Mustafa Unel, Vision based system identification and state estimation, *Springer Lecture Notes in Control and Information Sciences*, No. 237, 1998, 171-182.

[12] A. Mitiche, S. Seida and J. K. Aggarwal, Line based computation of structure and motion using angular invariance, *Proc. Workshop on Motion: Representation and Analysis*, IEEE Computer Society Press, Silver Spring, MD, 1986.

[13] Y. Liu and T. S. Huang, A linear algorithm for motion estimation using straight line correspondences, *Comput. Vision Graphics Image Process*, 44, 1988.

[14] M. E. Spetsakis and J. Aloimonos, Structure from motion using line correspondences, *Internat. J. Comput. Vision*, 4, 1990, 171-183.

[15] M. Jankovic and B. K. Ghosh, Visually guided ranging from observations of points, lines and curves via an identifier based nonlinear observer, *Systems and Control Letters*, 25, 1995, 63-73.

[16] N. Andreff, B. Espiau and R. Horaud, Visual servoing from lines, *Proc. of the 2000 IEEE International Conference on Robotics and Automation*, San Francisco, CA, April 2000, 2070-2075.

[17] R. Cipolla and A. Blake, Surface shape from the deformation of apparent contours, *Internat. J. Comput. Vision*, vol. 9, no. 2, 1992, 83-112.

[18] O. D. Faugeras, On the motion of 3-D curves and its relationship to optical flow, in: O.D.Faugeras, ed., *Proc. 1st ECCV* Springer, Berlin, 1990, 107-117.

[19] O. D. Faugeras and T. Papadopoulo, A theory of the motion fields of curves, *Internat. J. Comput. Vision*, vol. 10, no. 2, 1993, 125-156.

[20] K. S. Narendra, A. M. Annaswamy, *Stable Adaptive Systems*, (Prentice-Hall, Inc. 1989).

[21] T. Sahin and M. Unel, Globally Stabilized 3L Curve Fitting, *Lecture Notes in Computer Science*, vol. 3211, 2004, 495 - 502.